ELSEVIER

Available online at www.sciencedirect.com

ScienceDirect

Journal of Catalysis 255 (2008) 139–143

JOURNAL OF CATALYSIS

www.elsevier.com/locate/jcat

Priority Communication

Non-localized charge compensation in zeolites: A periodic DFT study of cationic gallium-oxide clusters in mordenite

Evgeny A. Pidko [a,*], Emiel J.M. Hensen [a], Georgy M. Zhidomirov [b], Rutger A. van Santen [a]

[a] *Schuit Institute of Catalysis, Eindhoven University of Technology, PO Box 513, NL-5600 MB Eindhoven, The Netherlands*
[b] *Boreskov Institute of Catalysis, Siberian Branch of the Russian Academy of Sciences, Novosibirsk, Russia*

Received 12 November 2007; revised 25 February 2008; accepted 25 February 2008

Abstract

Periodic DFT calculations show that stability of binuclear cationic gallium–oxo clusters in high-silica zeolites is mainly controlled by the favorable geometrical environment of the Ga^{3+} ions, whereas the effect of the direct interaction with the charge-compensating framework anionic sites is less important. Extraframework cyclic $Ga_2O_2^{2+}$ cations are shown to be active for light alkane dehydrogenation.

Keywords: Extraframework cations; Charge compensation; Zeolite; Gallium; Oxide clusters; Mordenite; Alkane dehydrogenation; Periodic DFT calculations

1. Introduction

Chemical reactivity of zeolites can be substantially affected by the presence of extraframework transition metal cations [1]. In order to understand their role in catalytic reactions insight into the molecular structure of these intrazeolitic species is desired. This however still remains a challenge in zeolite chemistry. For univalent cations, a well-accepted model is localization of the positively charged ions in the vicinity of the negatively charged framework aluminum-occupied oxygen tetrahedra [1]. For cations with a higher charge, this model requires close proximity of the aluminum substitutions in the zeolite framework. This requirement may not always be met, especially for high-silica zeolites such as MFI and mordenite, which are industrially important catalysts [1]. Recently, an alternative model has been put forward involving indirect charge compensation of Zn^{2+} ions by the negative ZSM-5 zeolite framework to account for the high reactivity of Zn/ZSM-5 zeolite in alkane activation [2]. The bivalent cation is placed in the vicinity of one framework anionic $[AlO_2]^-$ site, while the other negative framework site is located at a larger distance where it does not directly interact with the extraframework species. In spite of some spectroscopic [2] and theoretical [3] support, a firm basis for a model, in which the position of multivalent cations in zeolites is not dominated by localized charge compensation between the cation and the framework charge, is lacking. One notes however that indirect charge compensation is not uncommon in coordination compounds: a central metal ion is often surrounded by neutral ligands, while the charge-compensating anion is located outside the coordination shell [4]. To establish in more detail how charge compensation is accomplished in high-silica zeolites, we carried out a periodic DFT study of the interaction of isomeric bivalent $(GaO)_2^{2+}$ species with a model of zeolite mordenite (MOR, Si/Al = 23). We have recently shown that in oxidized Ga/ZSM-5 binuclear gallium-containing cationic species are the catalytically active clusters for alkane dehydrogenation [5]. It is not straightforward to see how these ions can be uniformly present in zeolites with a low Al content when the conventional charge-compensation model is followed. Therefore, we computed the structure of several $(GaO)_2^{2+}$ ions in mordenite with different Al distributions in the framework. The results indicate that our thinking of localization of multivalent cations in terms of direct charge compensation should be reconsidered.

Gallium-modified zeolites are effective catalysts for the aromatization of light alkanes [6]. Well-defined Ga cations in HZSM-5 can be prepared by the reaction of $Ga(CH_3)_3$ with

---

[*] Corresponding author. Fax: +31 40 245 5054.
E-mail address: e.a.pidko@tue.nl (E.A. Pidko).

0021-9517/$ – see front matter © 2008 Elsevier Inc. All rights reserved.
doi:10.1016/j.jcat.2008.02.027

Brønsted acid sites, resulting in grafted $Ga(CH_3)_2^+$ species [6b]. Careful removal of the methyl ligands leads to isolated Ga^+ ions. These ions dehydrogenate propane to propylene which is the first step in its aromatization. Further treatment of such Ga^+ ions with N_2O led to a considerable improvement of the catalytic activity, which was initially attributed to formation of isolated gallyl ions (GaO^+) [6b,7]. Recent theoretical studies have clearly shown that these species cannot be responsible for stable catalytic activity [8] and an alternative interpretation is the formation of extraframework oligomeric $(GaO)_n^{n+}$ species. The occurrence of cationic binuclear gallium–oxo clusters in ZSM-5 has been supported by EXAFS measurements and used to explain the enhancement of catalytic activity of Ga/ZSM-5 upon water co-feeding [5]. The important question here is whether proximate Al substitutions in the zeolite framework are necessary to stabilize these binuclear cationic species.

2. Computational details

The quantum-chemical calculations were carried out using Vienna Ab Initio Simulation Package (VASP) [9] within DFT with the gradient-corrected PW91 [10] exchange-correlation functional. The projected-augmented wave (PAW) method [11] was used to describe electron–ion interactions, and for valence electrons a plane wave basis set was employed. The energy cut-off was set to 400 eV. The Brillouin zone sampling was restricted to the Γ-point [12]. Cell parameters were initially optimized for the mordenite model. The parameters obtained were then used in all calculations. Full geometry optimizations were performed for each structure with the fixed cell parameters using a conjugated gradient algorithm. Convergence was assumed to be reached when the forces on each atom were below 0.05 eV/Å. A modest Gaussian smearing was applied to band occupations around the Fermi level ($\sigma = 0.1$ eV) and the total energies were extrapolated to $\sigma \to 0$.

The nudged elastic band method (NEB) [13] with improved tangent estimate was used to determine the minimum energy path and to locate the transition-state structures of elementary reactions involved in ethane dehydrogenation. The maximum energy geometries obtained with NEB method were then optimized separately using a quasi-Newton algorithm. In this step only positions of the atoms from Ga-containing extraframework intermediates and $[AlO_2]^-$ framework sites were optimized, while the remaining ions were fixed according to the positions obtained from the previous step.

The nature of the stationary point obtained was tested by analyzing the calculated harmonic normal modes, which were calculated using the finite difference method as implemented in VASP. Small displacements (0.02 Å) of atoms from the extraframework species and of the zeolitic ions directly bound to them were used for the estimation of numerical Hessian matrix. The rest of the zeolitic atoms were kept fixed to their equilibrium positions.

As detailed periodic DFT calculations with the large ZSM-5 unit cell are prohibitive in terms of computer demand, we choose mordenite as a model for a high-silica zeolite. Its purely siliceous structure has *Cmcm* space group symmetry. The orthorhombic cell of mordenite contains 144 atoms (48 Si and 96 O) [14]. It is possible, however, to choose a smaller lower symmetry monoclinic primitive cell of 72 atoms (24 Si and 48 O) [15] (Fig. 1a). After optimizing volume and shape, the parameters of the primitive cell are the following: $a = b = 13.648$ Å, $c = 7.508$ Å, and $\gamma = 97°$. These correspond to the cell parameters $a_1 = 18.087$ Å, $b_1 = 20.443$, $c_1 = 7.508$ of the conventional orthorhombic unit cell, which cohere well with the experimental XRD data [14]. To model a high-silica zeolite, a supercell was used. It was constructed by doubling the monoclinic unit cell along the c axis. The resulting cell contained 48 silicon atoms and 96 oxygens. To model gallium-exchanged mordenite two framework silicon ions were substituted with aluminums. The resulting models **I** and **II** (Figs. 1b and 1c, respectively) differ in framework Al distribution (Fig. 1d). In the case of model **I** both Al ions were located in one 8-membered ring connecting the main channel with the side-pocket of mordenite. In model **II** aluminum ions were located in the side-pockets opposite to each other in the main channel.

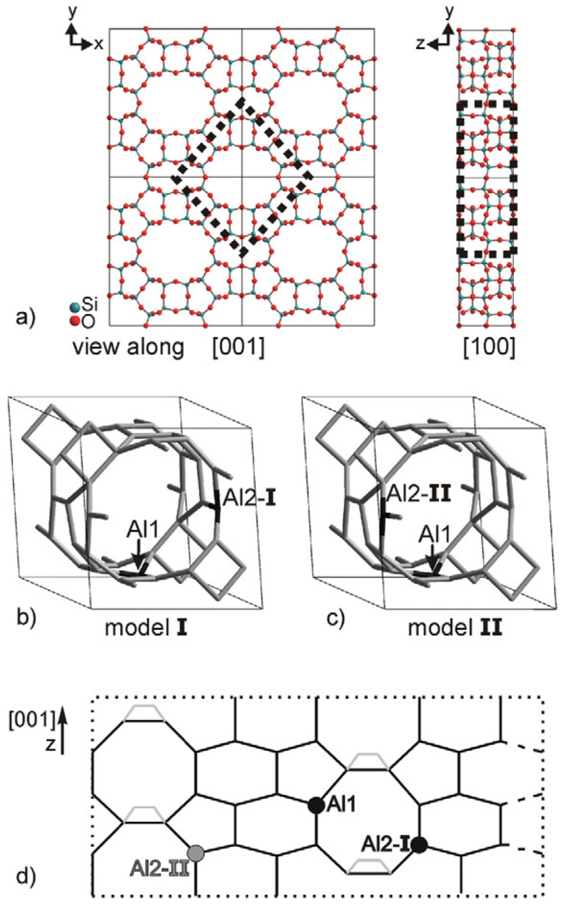

Fig. 1. Structure of mordenite (a) viewed along [001] and [100] (z and x axes, respectively). Orthorhombic and primitive monoclinic unit cells are shown, respectively, with solid and dashed lines. Supercell of high-silica mordenite models (b) **I** and (c) **II** (only silicon–aluminum framework is shown for clarity), and (d) their 2D schematic representation (the wall of the main channel of the mordenite supercell model was cut along [001] and rolled out). The locations of Al ions are shown as circles at appropriate positions in models **I** and **II**.

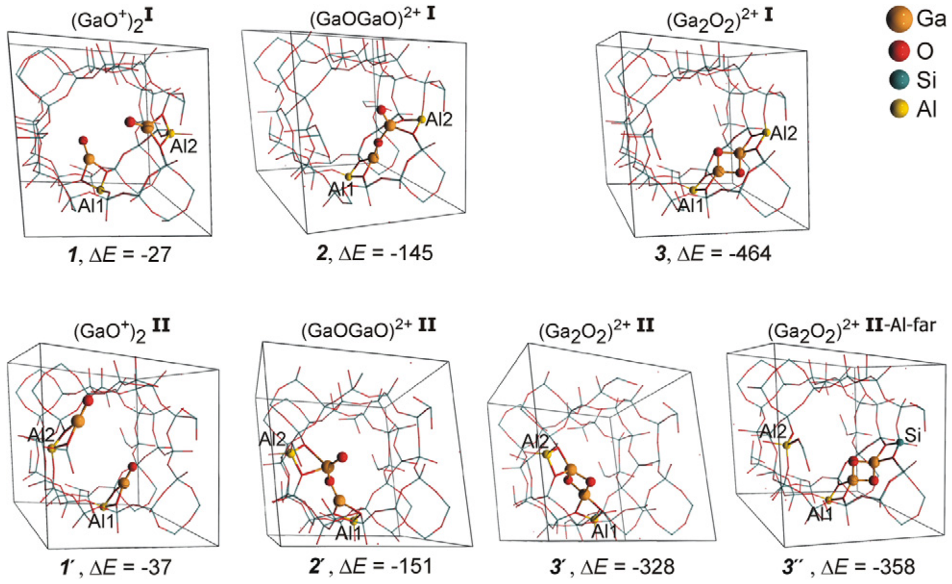

Fig. 2. Optimized structures of $(GaO)_2$ isomers stabilized in mordenite models **I** (upper row) and **II** (bottom row). The ΔE values (kJ/mol) correspond to the reaction energy for the stoichiometric oxidation of two exchangeable Ga^+ cations with N_2O toward the respective $(GaO)_2$ isomer according to the reaction $2Ga^+MOR + 2N_2O \rightarrow (GaO)_2^{2+}MOR + 2N_2$.

3. Results and discussion

Fig. 2 summarizes the stabilities of various $(GaO)_2^{2+}$ structures for the two models. The energy of the initial system with two Ga^+ ions does not depend on the Al distribution in the zeolite. Oxidation of the Ga^+ sites with N_2O to isolated GaO^+ (***1*** and ***1′***) ions is slightly exothermic. Formation of two isolated gallyl ions in a single side-pocket of MOR (***1***) requires a slightly unfavorable coordination of one of the GaO^+ cations to the zeolite wall. Geometry optimization of a similar starting structure but with both GaO^+ species initially coordinated to the oxygen anions of one 8T-ring of model **I** leads to structure ***2*** which is more stable by 118 kJ/mol. Similarly, rearrangement of the gallyl ions in model **II** results in the formation of an oxygen-bridged dimer ***2′*** with an energy benefit of 114 kJ/mol.

Further stabilization of the extraframework species is achieved by formation of an almost square-planar $(Ga_2O_2)^{2+}$ (***3*** and ***3′***) cation. This further lowers the total energies by 319 and 177 kJ/mol for models **I** and **II**, respectively. This relatively large difference between the two models is due to the formation of an almost perfect tetrahedral coordination of both Ga ions in the side-pocket of MOR in the case of ***3***. The less favorable coordination of structure ***3′*** is due to stabilization of $Ga_2O_2^{2+}$ along the zeolite channel that does not allow the favorable tetrahedral coordination around the Ga ions. This difference already points to the importance of optimal coordination around the Ga centers of the extraframework cationic complex. A more favorable location of the $(GaO)_2^{2+}$ ion in model **II** is obtained by allowing the complex to adopt tetrahedral coordination of Ga to oxygen anions in the side pocket (***3″***). The energy of this structure ***3″*** is lower by 30 kJ/mol, despite the separation of the charges: one Ga^{3+} ion coordinates to a neutral silicon-occupied oxygen tetrahedron and is located 5.441 Å away from the negative framework charge in the main channel. The favorability of such an unconventional charge compensation of a cationic complex derives from the dominance of the energy gain due to the stable tetrahedral surrounding of Ga^{3+} over the energy loss resulting from the lack of a counterion in the first coordination sphere of the metal center. It is important however to realize that the oxygen atoms ($O^{\delta-}$), which bridge between lattice silicons, are sufficiently basic to stabilize positively charged species.

Thus, the computations indicate that stabilization of the proposed binuclear gallium–oxo cations in high-silica zeolites is possibly independent of the Al distribution. The presence of such cationic Ga clusters is not surprising considering the large number of organometallic complexes of binuclear Ga centers. Indeed, a search of the Cambridge Structural Database [16] has revealed 139 different compounds containing a cyclic Ga_2O_2 moiety, whereas no crystal structure containing a terminal gallyl moiety was found. Most of these multinuclear compounds contain bis-(μ^2-OR)-di-gallium moieties (R = H, alkyl) analogous to those proposed in Ref. [5]. In addition, different polyhedron structures composed of such fragments have been described [17]. These bis-(μ^2-oxo)-di-gallium moieties can only be stabilized when chelating ligands coordinate to Ga [18]. In the present case, the zeolite framework can be considered a rigid polydentate ligand coordinating to the exchangeable cations.

Unlike ligands in solution, zeolites cannot adjust their structure significantly to provide the most effective stabilization of the intrazeolite cationic species. The dimensions of channel openings and cations sites of zeolites with different framework structures can differ from those of mordenite. Despite this, one expects that independently of the particular framework Al distribution, the rather large binuclear $Ga_2O_2^{2+}$ cations can coordinate to the $O^{\delta-}$-rich walls of high-silica zeolites with different morphologies in a variety of ways (not necessarily along the diameter of the zeolite channel) resulting in the stable tetrahe-

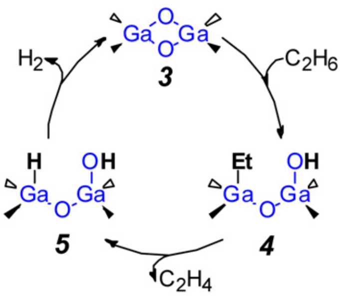

Scheme 1. Possible catalytic cycle for C_2H_6 dehydrogenation over binuclear gallium sites in mordenite (dangling bonds at Ga show coordination to zeolitic lattice oxygen anions).

Table 1
Calculated reaction (ΔE, kJ/mol) and activation energies ($\Delta E^{\ddagger}$, kJ/mol) for the heterolytic dissociation of C_2H_6 and recombination of H_2 over oxygenated Ga sites in mordenite

	ΔE	$\Delta E^{\ddagger}$
C–H bond activation		
$\boldsymbol{3} + C_2H_6 \rightarrow \boldsymbol{4}$	−62	118
$\boldsymbol{3''} + C_2H_6 \rightarrow \boldsymbol{4''}$ [a]	−76	n/a
$[GaO^+]MOR + C_2H_6 \rightarrow [Ga(C_2H_5)(OH)^+]MOR$	−258	69
H_2 recombination		
$\boldsymbol{5} \rightarrow \boldsymbol{3} + H_2$	92	168
$\boldsymbol{5''} \rightarrow \boldsymbol{3''} + H_2$	89	n/a
$[Ga(H)(OH)^+]MOR \rightarrow [GaO^+]MOR + H_2$	288	326

[a] Ga^{3+} coordinated to the $[AlO_2]^-$ framework unite was considered as the active site in the charge-alternating $Ga_2O_2^{2+}$ cation $\boldsymbol{3''}$.

dral or close to tetrahedral coordination of gallium ions. Thus, taking into account the above discussion and the extreme calculated stability of binuclear $Ga_2O_2^{2+}$ sites in mordenite, we conclude that such clusters should be predominant in oxidized gallium-containing high-silica zeolites with a Ga content close to the ion-exchange capacity.

In catalysis, the most stable sites often show significantly lower reactivity than lesser stable ones. To check whether this would also be the case for the Ga_2O_2 isomers, we calculated the energetics of the most important reaction steps (C–H bond activation and H_2 recombination) of catalytic dehydrogenation of ethane over the most stable structure ***3*** (Scheme 1) and over mononuclear GaO^+. For comparison the reaction energies for the respective elementary steps were computed for the charge-alternating structure $\boldsymbol{3''}$. The calculated reaction (ΔE) and activation energies ($\Delta E^{\ddagger}$) are summarized in Table 1.

Initial C–H bond cleavage of C_2H_6 over ***3*** is exothermic with a moderate activation barrier ($\boldsymbol{3} + C_2H_6 \rightarrow \boldsymbol{4}$). The calculated reaction energy of $\Delta E = -62$ kJ/mol is lower than that computed for dissociative chemisorption of ethane on isolated gallyl ion in **II** ($\Delta E = -258$ kJ/mol), while the difference in the activation energy barriers is much less pronounced (Table 1). Subsequently, the grafted $C_2H_5^-$ group decomposes to gas-phase ethylene and a hydride ion bound to Ga. This endothermic process depends only slightly on the nature of the Ga species [8]. Closure of the catalytic cycle by H_2 recombination from ***5*** is possible over the binuclear $Ga_2O_2^{2+}$ site ($\Delta E^{\ddagger} = 168$ kJ/mol, Table 1), whereas the barrier over the less stable isolated GaO^+ site is prohibitively high ($\Delta E^{\ddagger} = 326$ kJ/mol). The difference lies in the decreased basicity of the bridging extraframework oxygen anion. Thus, such bridging oxygens are essential to close the catalytic cycle by hydrogen recombination. One notes that the calculated reaction energies (Table 1) as well as the geometrical parameters of the intermediates (see Supplementary material) involved in the dissociative C_2H_6 adsorption and H_2 recombination over ***3*** and $\boldsymbol{3''}$ are very similar (Table 1). This suggests that the reactivity of the binuclear Ga sites depends only slightly on the mode of charge compensation.

In conclusion, cationic binuclear gallium–oxo clusters are more stable than isolated gallyl ions in high-silica zeolites and should be considered as active sites for light alkane dehydrogenation. Gallyl ions tend to oligomerize resulting in formation of oxygen-bridged Ga^{3+} pairs. The stability of such cationic binuclear complexes does not require proximate Al substitutions of the framework. The location and stability of such cationic clusters in the micropores is mainly controlled by the favorable coordinational environment around the Ga^{3+} centers. The effect of localized charge compensation is of lesser importance. Non-localized charge compensation is argued to be common in zeolites: the presence of multiply charged bi- or oligonuclear metal oxide species in zeolites does not require the immediate proximity of an equivalent number of negative framework charges.

Acknowledgments

The authors thank the European Union for financial support from the IDECAT framework. NWO-NCF is acknowledged for providing computational facilities.

Supplementary material

Details of structures discussed in the text are provided as supplementary material in the online version of this article.

Please visit DOI: 10.1016/j.jcat.2008.02.027.

References

[1] G. Centi, B. Wichterlova, A.T. Bell (Eds.), Catalysis by Unique Metal Ion Structures in Solid Matrices, NATO Science Series, Kluwer Academic, Dordrecht, 2001.

[2] (a) V.B. Kazansky, A.I. Serykh, Phys. Chem. Chem. Phys. 6 (2004) 3760;
(b) V.B. Kazansky, A.I. Serykh, E.A. Pidko, J. Catal. 225 (2004) 369;
(c) V.B. Kazansky, E.A. Pidko, J. Phys. Chem. B 109 (2005) 2103.

[3] (a) G.M. Zhidomirov, A.A. Shubin, V.B. Kazansky, R.A. van Santen, Theor. Chem. Acc. 114 (2005) 90;
(b) E.A. Pidko, R.A. van Santen, J. Phys. Chem. C 111 (2007) 2643, and references therein.

[4] Examples of crystal structures of Mg^{2+}, Ni^{2+} and Zn^{2+} complexes with indirect charge compensation can be found in (a) G. Meyer, M. Nolte, R. Berners, Z. Anorg. Allg. Chem. 632 (2006) 2184;
(b) T.F. Mastropietro, D. Armentano, N. Marino, G. De Munno, Cryst. Growth Des. 4 (2007) 609.

[5] E.J.M. Hensen, E.A. Pidko, N. Rane, R.A. van Santen, Angew. Chem. Int. Ed. 46 (2007) 7273.

[6] (a) A. Hagen, F. Roessner, Catal. Rev. 42 (2000) 403;
(b) N. Rane, A.R. Overweg, V.B. Kazansky, R.A. van Santen, E.J.M. Hensen, J. Catal. 239 (2006) 478, and references therein.

[7] N.O. Gonzales, A.K. Chakraborty, A.T. Bell, Top. Catal. 9 (1999) 207.

[8] E.A. Pidko, E.J.M. Hensen, R.A. van Santen, J. Phys. Chem. C 111 (2007) 13068.

[9] G. Kresse, J. Furthmüller, Comp. Mat. Sci. 6 (1996) 15;
G. Kresse, J. Furthmüller, Phys. Rev. B 54 (1996) 11169.

[10] J.P. Perdew, J.A. Chevary, S.H. Vosko, K.A. Jackson, M.R. Pederson, D.J. Singh, C. Fiolhais, Phys. Rev. B 46 (1992) 6671.

[11] P.E. Blöchl, Phys. Rev. B 50 (1994) 17953;
G. Kresse, J. Joubert, Phys. Rev. B 59 (1999) 1758.

[12] H.J. Monkhorst, J.D. Pack, Phys. Rev. B 13 (1976) 5188.

[13] G. Mills, H. Jónsson, G.K. Schenter, Surf. Sci. 324 (1995) 305.

[14] P.R. Rudolf, J.M. Garcés, Zeolites 14 (1994) 137.

[15] (a) X. Rozanska, R.A. van Santen, F. Hutschka, J. Hafner, J. Am. Chem. Soc. 123 (2001) 7655;
(b) R. Grybos, J. Hafner, L. Benco, H. Toulhoat, J. Phys. Chem. C 111 (2007) 6454.

[16] CSD (version 5.28), November 2006 update release.

[17] M. Albrecht, S. Dehn, R. Frönlich, Angew. Chem. Int. Ed. 45 (2006) 2792;
P. Hodge, B. Piggott, Chem. Commun. (1998) 1933;
G. Linti, G. Li, H. Pritzkow, J. Organomet. Chem. 626 (2001) 82;
P.J. Nichols, S. Papadopoulos, C.L. Raston, Chem. Commun. (2000) 1227, and references therein.

[18] R.J. Baker, C. Jones, M. Kloth, Dalton Trans. (2005) 2106.